CONF-920927--2

UCRL-JC--109658

DE93 009547

Electronic Structure Theory of Alloy Phase Stability

P.E.A. Turchi
M. Sluiter

This paper was prepared for submittal to
CAMSE '92, Yokohama, Japan
September 22-25, 1992

August 24, 1992

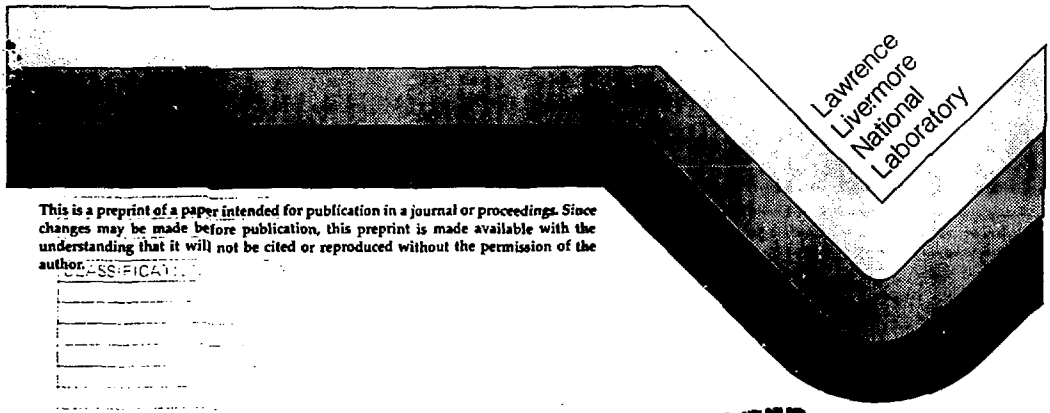

Electronic structure theory of alloy phase stability

P. E. A. Turchi and M. Sluiter [a] *

[a]Lawrence Livermore National Laboratory, Condensed Matter Division (L-268), Livermore, CA 94550, USA

We present a brief overview of the advanced methodology which has been developed and applied to the study of phase stability properties in substitutional alloys. The approach is based on the real space version of the Generalized Perturbation Method within the Korringa-Kohn-Rostoker multiple scattering formulation of the Coherent Potential Approximation. Temperature effects are taken into account with a generalized meanfield approach, namely the Cluster Variation Method, or with Monte-Carlo simulations. We show that this approach is well suited for studying ground state properties of substitutional alloys, for calculating energies of idealized interfaces and antiphase boundaries, and finally to compute alloy phase diagrams.

1. INTRODUCTION

Besides providing thermodynamic data to alloy designers solely on the basis of phenomenological models, considerable efforts have been put in recent years on trying to address the problem of alloy phase stability from a first-principles electronic structure approach. Starting with an assembly of nuclei and electrons which characterizes an alloy, the electronic structure properties are well described within the Local Density Functional theory [1]. On the other hand, order-disorder phenomena in alloys are expressed for an assembly of site occupancies by an Ising-like Hamiltonian:

$$H = \sum_{m,n} \epsilon_{mn}\sigma_m\sigma_n + \sum_{l,m,n} \epsilon_{lmn}\sigma_l\sigma_m\sigma_n + \cdots \quad (1)$$

where ϵ_{mn}, ϵ_{lmn}, $\cdots$ represent two, three, $\cdots$ body interaction energies and σ_n is a spin-like variable which takes, for a binary alloy, the value +1 or -1 depending on whether or not a B species occupies site n. By mapping the original assembly of nuclei and electrons onto an assembly of spin-like variables, with the physics of the former system transferred into the interaction energies of the latter, the following question: "what kind of ordered configuration (if any) and crystalline structure an alloy will choose as a function of concentration, temperature and pressure ?", may be addressed. Among the possible methods which provide such mapping, one should mention the Generalized Perturbation Method (GPM), first introduced by Ducastelle and Gautier [2], the Embedded Cluster Method (ECM) of Gonis et al. [3, 4], the Concentration Functional Theory (CFT) of Györffy and Stocks [5], the latter being a k-space approach contrary to the first two methods which are developed in real space. These three methods differ in spirit from the so-called Connolly-Williams Method (CWM) [6] which does not address this difficult mapping issue, but instead assumes it. The first three methods rely on the knowledge of the electronic structure properties of the random configuration of the alloy, taken as a reference medium, whereas the CWM approach essentially deals with ordered alloy configurations. In what follows, we will mostly focus on the GPM and its applications.

In the GPM context, starting from a detailed description of the reference medium, within for example the Coherent Potential Approximation (CPA) [7, 8], one describes the energy of a given configuration C of an alloy $A_{1-c}B_c$ based on a specific underlying lattice, and defined by a set of occupation numbers p_n (p_n takes the value 1 if site n is occupied by a B species, 0 otherwise), by the sum of two terms:

$$\Delta E^{\mathbf{C}} = \Delta E_{\mathrm{Mix}} + \Delta E^{\mathbf{C}}_{\mathrm{Ord}} \quad (2)$$

where

$$\Delta E_{\mathrm{Mix}} = E^T_{CPA} - (1-c)E^T_A - cE^T_B \quad (3)$$

*Work performed under the auspices of the U.S. Department of Energy by the Lawrence Livermore National Laboratory under Contract No. W- 7405-Eng-48. Part of this work was performed in collaboration with G. M. Stocks (ORNL) who is gratefully acknowledged.

is the mixing energy of the alloy given by the difference between the total energy of the random medium and the concentration weighted average of the total energies of the pure species. This contribution is obviously concentration-dependent but configuration-independent. The second term in Eq.(2) is the so-called ordering energy which is concentration- and configuration-dependent, and takes within the GPM context the following form:

$$\Delta E^{\mathbf{C}}_{\mathrm{Ord}}(\{\delta c_n\}) = \sum_{k=2}^{\infty} \frac{1}{k} \sum_{n_1,n_2,\cdots,n_k} V^{(k)}_{n_1 n_2 \cdots n_k} \delta c_{n_1} \times \delta c_{n_2} \cdots \delta c_{n_k} \quad (4)$$

where $\delta c_n = p_n - c$ represents the fluctuation of local concentration around the average concentration of the random medium, and the sum runs over different consecutive site indices n_i. The set of V's refers to the effective cluster interactions (ECI's). To lowest order in perturbation, the expansion in Eq.(4) can be rewritten as:

$$\Delta E^{\mathbf{C}}_{\mathrm{Ord}} \simeq \sum_s q^{\mathbf{C}}_s V_s \quad (5)$$

where $q^{\mathbf{C}}_s$ specifies the configuration. Indeed, by definition:

$$q^{\mathbf{C}}_s = \frac{c}{2}(n^{\mathrm{BB}}_s - c n_s) \quad (6)$$

where n^{BB}_s and n_s refer to the number of BB pairs and total number of pairs, per site, between an atom at the origin and the other in the s^{th} neighbor shell. V_s is an effective pair interaction (EPI) given by the combination:

$$V_s = V^{\mathrm{AA}}_s + V^{\mathrm{BB}}_s - 2V^{\mathrm{AB}}_s \quad (7)$$

Table 1 lists q_s values for some typical superstructures. Note that according to its definition, a positive (negative) V_s indicates that AB (AA or BB) pairs between an atom at the origin and the others in the s^{th} neighbor shell are favored. The expansion given in Eq.(5) is simply rewritten in an Ising-like form by replacing p_n by the spin-like variable σ_n, $\sigma_n = 2p_n - 1$:

$$\Delta E^{\mathbf{C}}_{\mathrm{Ord}} \simeq -\frac{1}{2}\sum_s n_s (2c-1)^2 \frac{V_s}{4} + \frac{1}{2N}\sum_{m,n\neq m} \frac{V_{mn}}{4}\sigma_m\sigma_n \quad (8)$$

Contrary to what is done within the CWM approach, the Ising-like expression which will carry all the information on order-disorder phenomena is associated with one of the contributions to the total energy of a configuration C, namely $\Delta E^{\mathbf{C}}_{Ord}$ in the GPM context, see Eq.(2), and not $\Delta E^{\mathbf{C}}$ as assumed in the CWM. Note that no formal proof exists of the validity of an Ising-like expansion for the total energy of an alloy, and the basic asumption made in the CWM has to be checked out for every alloy case by a careful numerical analysis. In addition, the CWM being essentially a grand canonical approach to the problem of stability in alloys, this method brings into question the meaning of convergence of an expansion similar to Eq.(1), as this equation presumably converges at different rates, if at all, for alloy configurations at different compositions.

Besides providing a formal proof of the validity of an Ising-like Hamiltonian to describe ordering processes in alloys, the GPM guarantees a rapid convergence of the expansion given by Eqs.(4), (5) or (8) in terms of effective pair and cluster interactions, a property which shows that the "CPA medium" defines an appropriate reference. By performing such a perturbation from a medium which is inherently concentration-dependent, the interactions are concentration-dependent, thus leading to a 3-dimensional generalized Ising Hamiltonian, that is able to describe a much broader spectrum of physical phenomena than the one originally studied by Ising. In the following, the electronic structure properties of the disordered medium are based upon the charge self-consistent Korringa-Kohn-Rostoker - Coherent Potential Approximation (KKR-CPA) muffin-tin potentials with an angular momentum extending up to l=3, and the EPI's are calculated with the GPM approach from the KKR-CPA medium [9].

With those interactions, one can predict the most probable ordered configuration of an alloy at each composition, by referring to the ground state analysis of the Ising model established for the appropriate lattice (see Ref. [7] for a review). Such results are usually summarized in so-called ground state ordering maps which indicate, in

Table 1
q_s-values entering Eq.(5) for some typical ordered structures (Struktur Bericht's notation).

Ordered Phase	q_1	q_2	q_3	q_4	q_5	q_6	q_7
bcc – B2	-1	3/4	3/2	-3	1	3/4	-3
bcc – B32	0	-3/4	3/2	0	-1	3/4	0
bcc – B11	0	1/4	-1/2	0	-1	3/4	0
bcc – DO_3	-1/4	-3/16	9/8	-3/4	-1/4	9/16	-3/4
fcc – LI_0	-1/2	3/4	-1	3/2	-1	1	-2
fcc – LI_1	0	-3/4	0	3/2	0	-1	0
fcc – $MoPt_2$	-1/3	0	2/3	-1/3	0	2/9	-4/3
fcc – LI_2	-3/8	9/16	-3/4	9/8	-3/4	3/4	-3/2
fcc – DO_{22}	-3/8	5/16	1/4	1/8	-3/4	-1/4	1/2

the space spanned by the EPI's, the domains of stability of each ordered superstructure. These most probable ordered superstructures may also be confirmed by Monte-Carlo simulations, provided some care is taken on the size of the simulation box and on the application of the boundary conditions.

It is important to point out that a general answer to the problem of phase stability, even at zero temperature, requires the knowledge of the ordering part of the total energy of an alloy in the entire range of composition, and also, because of the way the configuration energy ΔE^{C}, in Eq.(2) was expressed, of the mixing energy at every composition. In addition, by examining all possible configurations on a fixed crystalline structure, we exclude the possibility that an ordered state based on a different lattice may be more stable. Meanwhile, the above treatment provides a useful answer to the determination of the most probable (i.e. metastable, if not stable) ground states on a fixed lattice, at each stoichiometry. A general understanding of the origin of chemical order in alloys may be gained by studying in more details the critical role played by the number of valence electrons of the alloy constituents as well as the nature of the electronic states which contribute to bond order and strength in substitutional alloys. For transition metal alloys, these first-principles studies confirm as far as trends are concerned, previous results established on the basis of semi-phenomenological tight-binding calculations [7].

Another application of this approach is the calculation of antiphase boundary (APB) and interfacial energies. APB's result from the motion of dislocations in ordered structures, and their energy is a measure of how easy the defect can move through the crystal. APB's are characterized by two parameters: the crystallographic plane which defines the boundary, and the displacement vector associated with the burgers vector of the dislocation [10]. Although relaxations near the boundary may play an important role (APB energies may be reduced in some cases by more than 40%, see e.g. Ref. [11]), the calculation for unrelaxed boundaries is a good indicator of mechanical behavior. The APB energy takes the following form:

$$E_{\mathrm{APB}}(p,d) = \frac{1}{S_p} \sum_s \alpha_s(p,d) V_s \qquad (9)$$

where p and d denote the plane and the displacement vector of the APB, S_p is the surface area per atom on the p plane, the sum runs over neighbor shells, and $\alpha_s(p,d)$ is a geometric coefficient which can be determined from the number of neighbor pairs which have been changed from AA or BB type to AB type, per unit area (see Table 2). The treatment of idealized interfaces (i.e. without roughness) can be performed similarly to that of APB's. By definition, the interfacial plane separates a halfcrystal of pure A from a halfcrystal of pure B. Once again, if topological disorder near the interface is ignored, the interfacial energy is given by an expression similar to Eq.(9) in which the α_s only depend on the interface orientation p (see Table IV in Ref. [12] for an explicit evaluation of these parameters).

Table 2
α_s-values and surface areas S (in units of a^2, where a is the lattice parameter), which enter Eq.(9) for describing APB energies in B2 and LI_2. The * denotes the average of two non-conservative APB's.

p	d	α_1	α_2	α_3	α_4	α_5	α_6	α_7	S
110	$1\bar{1}1$	1	-1	-3	7	-2	- 2	9	$\sqrt{2}/2$
211	$1\bar{1}\bar{1}$	2	-2	-5	12	-4	- 4	16	$\sqrt{6}/2$
310	$1\bar{3}1$	3	-2	-7	15	-6	- 4	21	$\sqrt{10}/2$
100*	111*	2	-1/2	-2	6	-2	- 1/2	6	1
111*	$11\bar{1}$*	3	-3	-6	18	-6	- 6	21	$\sqrt{3}$
100	$0\bar{1}1$	0	-1/2	2	-2	0	- 2		1/2
110	$1\bar{1}0$	1/2	-1	1	-3	3	- 2		$\sqrt{2}/2$
311	$0\bar{1}1$	1/4	-5/4	3	-7/2	3/2	- 3		$\sqrt{11}/4$
111	$1\bar{1}0$	1/4	-3/4	1	-3/2	3/2	- 3/2		$\sqrt{3}/4$
102	$\bar{2}11$	1	-3/2	2	-5	4	- 4		$\sqrt{5}/2$
112	$1\bar{1}0$	1/2	-2	4	-5	3	- 4		$\sqrt{6}/2$
310	$1\bar{3}0$	3/2	-2	3	-7	6	- 6		$\sqrt{10}/2$
510	$1\bar{5}0$	5/2	-3	5	-11	10	- 10		$\sqrt{26}/2$

Finally, the thermodynamics of substitutional alloys can be studied by solving the Ising Hamiltonian at finite temperature. The most popular methods are the Cluster Variation Method (CVM) [13], based on a generalized meanfield theory, and Monte-Carlo simulations. A broad selection of properties can thereby be calculated, in particular: short- and long-range order parameters, short-range order induced diffuse scattering, order-disorder temperatures, and ultimately composition-temperature-pressure phase diagrams.

Several applications of the advanced scheme (see Ref. [14] for a general flow chart) are briefly presented in the next section.

2. APPLICATIONS

We summarize some of the results obtained for Ni-Al. Among the important features of the phase diagram [15], it is worth mentioning: the large domain of stability around equicomposition of a bcc-based B2 phase of CsCl-type which melts before disordering; at Ni_3Al, a fcc-based LI_2 phase of Cu_3Au-type is found stable; at low Ni content (below 50 at.% Ni) the system exhibits line compounds with complex phases and almost no solubility of Ni in Al (it is acknowledged that stability is accommodated by vacancy formation), whereas at high Ni content, a fcc solid solution is stabilized. Among the phenomena of metallurgical interest, one should mention the martensitic transformation taking place around 62 at.% Ni in a narrow range of composition, at the proximity of the existence of an ordered phase Ni_5Al_3 of Pt_5Ga_3-type based on a bct structure. We now discuss to what extent these experimental observations can be understood and even predicted with the first-principles approach outlined above.

A first understanding of the phase stability properties of this alloy derives from inspection of the energy of mixing curves (see Fig. 1a). The endpoints of the curves indicate that the pure elements are more stable on the fcc than on the bcc lattice, in accordance with experimental fact. The energies of mixing on both the fcc and bcc lattices are strongly negative, indicating that alloy formation, even in the random state, is much favored over phase separation. By inspecting the curvature of the mixing energy curves for both fcc- and bcc-based disordered alloys, note that the downward curvature at the Ni-rich side strongly suggests a fair solubility of Al in Ni, whereas the upward curvature at the Al-rich side indicates that the solubility of Ni in Al is very limited. In

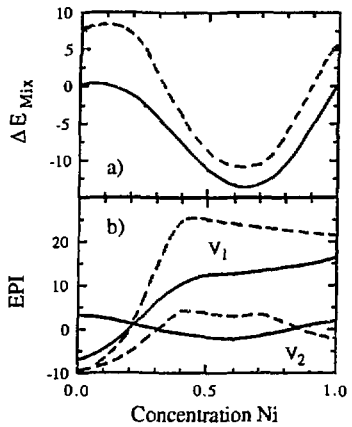

Figure 1. a) Mixing energies (fcc-based Ni and Al are taken as references), and b) EPI's, in mRy/atom, as a function of Ni concentration, for fcc- (solid curve) and bcc- (dashed curve) based Ni-Al alloys (see also Refs. [20,21]).

fact, it appears that at the Al-rich side the lowest energies can be attained by a phase separation between pure Al and a phase with approximate composition NiAl. Therefore, the occurrence of fcc or bcc based structures in that composition range is unlikely.

The EPI's obtained from the KKR-CPA-GPM approach for Ni-Al converge rapidly with distance, and the multi-site interactions are negligible. The nearest neighbor EPI's on both the fcc and bcc lattice (see Fig. 1b) show similar features: they are negative at the Al-terminal point, increase with Ni-content until the equiatomic composition is reached, and then remain nearly constant and positive with further increases in Ni-content. The negative interactions in Al-rich alloys indicate that no stable ordered phase can occur. Oftentimes, when ordering tendencies are weak, phases with complex crystalline structures occur.

Together with the results of the ground state properties of the Ising model for the fcc lattice up to 4th neighbor shell [16] and for the bcc one up to the 5th neighbor shell but with V_4 excluded [17], the most probable ordered superstructures can be predicted. On the fcc lattice the most probable compounds are: NiAl with an LI_0 crystal structure, and Ni_3Al with the LI_2 structure. On the bcc lattice three phases are possible: NiAl with the B2 structure; Ni_5Al_3 with a phase "9" type of structure according to the notations of Ref. [17] which closely approximates the ordered structure of Pt_5Ga_3 seen experimentally on a bct structure; and Ni_2Al with a DO_3 structure. When the structural energy difference between bcc and fcc is considered [18] for the pure elements it is evident that for NiAl B2 is much more stable than LI_0, whereas for Ni_3Al LI_2 is more stable than DO_3. For intermediate compositions between NiAl and Ni_3Al, we find that the fcc and bcc-based structures are almost equally stable. Based on entropy arguments [14], it is anticipated that in a narrow range of composition, the high temperature bcc phase will transform in a low temperature fcc phase, and such a phenomenon gives rise to martensitic transformations which occur in actual Ni-Al alloys with compositions of about 62.5 at.% Ni [19]. In that alloy we have predicted a bcc-based superstructure, phase "9", which has been shown to be almost identical with the actually occurring structure of Pt_5Ga_3 type [20]. The latter is based on a bct lattice, which is an interpolation between the fcc and bcc lattices, as one would expect on the basis of the first-principles results.

At finite temperature, the energetic quantities displayed in Fig. 1 can be used with a statistical thermodynamic description of the Ising model, namely the CVM [13] (see also [21] for further details) to evaluate the configurational free energy as a function of concentration. The calculated Ni-rich portion of the Ni-Al phase diagram is displayed in Fig. 2. The agreement with the experimental phase diagram in terms of phase occurences and phase boundaries is quite satisfactory. The only shortcomings of our approach

are that we do not have a theoretical framework that allows us to consider the liquid phase, nor can we at present properly include the Ni_5Al_3 phase on the bct lattice. Note that the bcc-approximant of this latter phase (referred to as "9" in Fig. 2) is found stable at very low temperature and slightly off-stoichiometry, and taking into account the tetragonal distortion of the lattice should correct for the discrepancy. Since features in the phase diagram are extremely sensitive to minor inaccuracies in the free energy, we conclude that our approach produces a fairly accurate description of the energetics of Ni-Al alloys. In particular, our study reveals a possible relation between the martensitic transformation and the stability of an ordered phase around Ni_5Al_3, and also the existence of metastable phases (such as Ni_3Al with the DO_3 structure) that are not readily available from experiment.

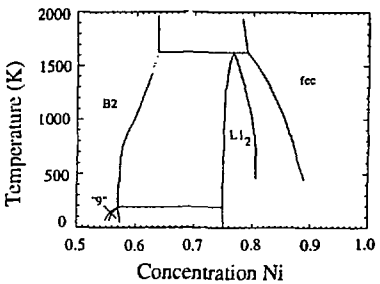

Figure 2. Ni-rich portion of the computed Ni-Al phase diagram.

To further validate the approach, the EPI's can be compared with the ones deduced from short range order scattering intensity measurements, especially in a region of the phase diagram where a solid solution exists. In Ni-Al, the measurements are limited to high Ni-content, above 90 at.% Ni. Our EPI's compare well with the results of Ref. [22], and are within the error bars of other experimental values [23]. Consequently, our diffuse scattering intensities computed with the CVM approach are in remarkable agreement with experiments [20]. Note that the same methodology was recently applied with an equal success to a similar system, Cu- Zn [24], and also to a phase separating case, Pd-Rh [25].

Other applications of our first-principles description of Ni-Al alloys include the computation of APB and interfacial energies. For comparison, we also present the results for Cu-Zn alloys. Table 3 lists APB energies for NiAl and Ni_3Al on a number of low-index planes. The APB energies in B2-NiAl and CuZn are anisotropic and the (110) planes are much favored over the other low-index planes. Since the APB energies scale with the ordering energy of this alloy configuration, they are larger for NiAl than CuZn. The discrepancy which is usually observed between theoretical estimates and experimentally deduced APB energies can be attributed to essentially three factors: relaxation effects already mentioned, less than perfect long range order, and partial disorder along the APB. Meanwhile, in the case of

Table 3
Computed APB energies γ (in mJ/m^2) in B2 and $L1_2$ Ni-Al and Cu-Zn alloys. In the case of non-conservative APB's, designated by *, the average was taken over a conservative pair of APB's.

phase	APB − type	γ_{Ni-Al}	γ_{Cu-Zn}
B2 − phase	(110)	748	69
	(211)	879	86
	(310)	1093	118
	(100)*	1238	163
	(111)*	936	97
$L1_2$ − phase	(100)	196	25
	(110)	296	52
	(111)	283	48
	(210)	354	60
	(310)	369	62
	(510)	375	62
	(211)	279	44
	(311)	265	40

β-CuZn, the magnitude of the APB energies compare reasonably well with other evaluations [26]. In the case of LI_2-Ni_3Al, for which case experimental data are available, the ratio of the (111) APB energy over the (100) one, equal to 1.44 (see Table 3), is found very close to the value of 1.2 estimated from experiments [27]. Other theoretical investigations [28] which do ignore the effects mentioned above find values of APB energies quite comparable to the ones presented here. These calculations are useful to predict the most probable APB's at each composition, and their behavior at finite temperature [29, 30].

The pair interactions can be used to compute the interfacial energy according to Eq.(9). The results for some alloys and low-index interface orientations are listed in Table 4. As expected,

Table 4
Interfacial energies, in mRy/a^2, where a is the lattice parameter, for some equiatomic bcc-based alloys, and for some low-index planes.

Alloy	CuZn	NiTi	NiAl	AlLi
100	-9.1	-15.5	-57.0	-7.4
110	-7.4	-17.4	-44.4	-13.7
111	-8.6	-18.0	-52.4	-17.4
311	-8.9	-16.8	-57.1	-13.1
331	-8.2	-18.1	-49.6	-15.4
210	-8.8	-16.7	-53.2	-11.0

systems that exhibit ordering tend to have negative interfacial energies, indicating that such interfaces are energetically favorable. As illustrated in Table 4, it is generally observed that the interfacial energy is rather insensitive to a particular interface orientation. This property originates from the weak orientation-dependence of the $\alpha_s(p)/S_p$ ratio in Eq.(9), and holds even in cases where the interactions are very short ranged [12]. This means that in those systems where chemical effects at the interface are dominant, precipitates will tend naturally to exhibit a spherical shape regardless of whether the EPI's are short or long ranged. Therefore, the occurrence of nearly spherical precipitates in alloys where misfit strains are small, as in the case of Al-rich Al-Li alloys with Al_3Li precipitates, is not an indication of the presence of long range interactions.

3. CONCLUSION

The methodology we briefly reviewed in this paper provides a theoretical framework for the study of chemical order effects in alloys. Applications to a wide variety of subject areas not only confirm known experimental results, but also explain in terms of basic parameters the origin of alloy stability. The multiple scattering formalism on which the GPM is based is well suited to address stability issues in multi-component systems or superlattices [12] and also in materials with reduced symmetry, such as at surfaces, and to study the coupling between magnetic and chemical order in alloys. There is now a need to incorporate this approach in a more general framework to account for dynamical effects, and thus to address in its generality structural and chemical effects on the stability of metals and alloys.

REFERENCES

1 W. Kohn and L.J. Sham, Phys. Rev. B140 (1965) A1133.
2 F. Ducastelle and F Gautier, J. Phys. F6 (1976) 2039.
3 A. Gonis, X.-G. Zhang, A.J. Freeman, P.E.A. Turchi, G.M. Stocks and D.M. Nicholson, Phys. Rev. B36 (1987) 4630.
4 A. Gonis, M. Sluiter, P.E.A. Turchi, G.M. Stocks and D.M. Nicholson, J. Less Com. Met. 168 (1991) 127.
5 B.L. Györffy and G.M. Stocks, Phys. Rev. Lett. 50 (1983) 374.
6 J.W.D. Connolly and A.R. Williams, Phys. Rev. B27 (1983) 5169.
7 F. Ducastelle, *Order and Phase Stability in Alloys*, F. R. de Boer and D. G. Pettifor eds. (North-Holland, Amsterdam, 1991), *Cohesion and Structure* series, vol. 3.
8 J.S. Faulkner, Progress in Materials Science 27 (1982) 1 ; and references cited therein.
9 P.E.A. Turchi, G.M. Stocks, W.H. Butler, D.M. Nicholson and A. Gonis, Phys. Rev.

B37 (1988) 5982.
10 G. Inden, S. Bruns and H. Ackermann, Phil. Mag. A55 (1986) 283; T. Kawabata and O. Izumi, Phil. Mag. A55 (1987) 823.
11 P. Beauchamp, J. Douin and P. Veyssière, Phil. Mag. A55 (1987) 565.
12 M. Sluiter and P.E.A. Turchi, Phys. Rev. B46 (1992) 2565.
13 R. Kikuchi, Phys. Rev. 81 (1951) 988; J.M. Sanchez, F. Ducastelle and D. Gratias, Physica A128 (1984) 334.
14 P.E.A. Turchi, Mater. Sci. and Eng. A127 (1990) 145 ; and references cited therein.
15 *Binary Alloy Phase Diagrams*, T.B. Massalski ed. (ASM International, Materials Park, OH, 1990), vols. 1 to 3.
16 J. Kanamori and Y. Kakehashi, J. Phys. (Paris), Colloq. 38 (1977) C-7-274.
17 A. Finel and F. Ducastelle, *Phase Transformations in Solids*, T. Tsakalakos ed. (North-Holland, Amsterdam, 1984), p. 293; A. Finel, Thèse de Doctorat d'Etat es Sciences Physiques, University Paris VI, 1987 (unpublished), and ONERA Report #1987-3.
18 N. Saunders, A.P. Miodownik and A.T. Dinsdale, Calphad 12 (1988) 351.
19 Y. Noda, S.M. Shapiro, G. Shirane, Y. Yamada and L.E. Tanner, Phys. Rev. B42 (1990) 10397.
20 M. Sluiter, P.E.A. Turchi, F.J. Pinski and G.M. Stocks, Mater. Sci. and Eng. A152 (1992) 1.
21 M. Sluiter and P.E.A. Turchi, in these Proceedings.
22 F. Klaiber, B. Schönfeld and G. Kostorz, Acta Cryst. A43 (1987) 525.
23 F. Chassagne, M. Bessière, Y. Calvayrac, P. Cénédèse and S. Lefebvre, Acta Metall. 37 (1989) 2329.
24 P.E.A. Turchi, M. Sluiter, F.J. Pinski, D.D. Johnson, D. M. Nicholson, G.M. Stocks and J.B. Staunton, Phys. Rev. Lett 67 (1991) 1779: Erratum 68 (1992) 418.
25 D.D. Johnson, P.E.A. Turchi, M. Sluiter, D.M. Nicholson, F.J. Pinski and G.M. Stocks, MRS Symp. Proc. , vol. 186 (1991) 21.
26 H. Saka, M. Kawase, A. Nohara and T. Imura, Phil. Mag. A50 (1986) 65; and references cited therein.
27 M.H. Yoo, Acta Metall. 35 (1987) 1559.
28 J. Douin, P. Veyssière and P. Beauchamp, Phil. Mag. A54 (1986) 375.
29 P. Beauchamp, G. Ditras and P. Veyssière, Phil. Mag. A65 (1992) 477.
30 A. Finel, V. Mazauric and F. Ducastelle, Phys. Rev. Lett. 65 (1990) 1016.